



AN ASSESSMENT OF SITE AMPLIFICATION FACTORS FOR THE WESTERN UNITED STATES

Yin-Nan Huang¹, Andrew S. Whittaker² and Nicolas Luco³

ABSTRACT

The Next Generation Attenuation (NGA) ground motion relationships enable an assessment of the site class coefficients presented in the 2003 NEHRP Provisions and ASCE-7-05 for the Western United States. A site amplification study is performed using the three NGA relationships used by the USGS to update their seismic hazard maps for the Western United States. The average NGA site amplification factors show a clear dependency on period for average shear-wave velocity smaller than 270 m/s; can vary significantly within a site class (D or E) for a given bedrock spectral intensity in the mid- and long-period ranges; and are substantially greater than the current NEHRP/ASCE-7 site class coefficients in some cases.

Introduction

The procedure for developing site-specific design spectra in the 2003 *NEHRP Recommended Provisions for Seismic Regulations for New Buildings and Other Structures* (FEMA 2004) and ASCE Standard 7 *Minimum Design Loads for Buildings and Other Structures* (ASCE 2006) involves the use of short- and 1-second-period site class coefficients, F_a and F_v , to amplitude scale the short- and 1-second-period bedrock mapped acceleration parameters, S_s and S_1 , respectively. The NEHRP/ASCE-7 site class coefficients are based in a large part on the seminal studies of Borchardt (1994) using a reference shear wave velocity of 1050 m/s for the uniform site condition. He reported the average ratios of Fourier spectra between soil and nearby rock sites using strong-motion records from the 1989 Loma Prieta earthquake and provided a basis for the site class coefficients at a bedrock peak ground acceleration (PGA) level of about 0.1 g. The site class coefficients at higher values of PGA are based on the results of parametric studies using one-dimensional site response analysis techniques calibrated using empirical estimates from records of the Loma Prieta earthquake (Seed et al. 1994; Dobry et al. 1994).

The development of the Next Generation Attenuation (NGA) relationships permits an assessment of the site class coefficients presented in the 2003 *NEHRP Provisions* and ASCE-7-

¹Assistant Professor, Division of Structures and Mechanics, School of Civil and Environmental Engineering, Nanyang Technological University, Singapore 639798

²Professor, Dept. of Civil, Structural and Environmental Engineering, State University of New York at Buffalo, Buffalo, New York, United States

³Research Structural Engineer, United States Geological Survey, Denver, Colorado, United States

05 for the Western United States. The ground-motion database used in the NGA project includes 173 earthquakes, 1456 recording stations and 3551 records (Power et al. 2008). The United States Geological Survey (USGS) has used three NGA relationships, namely, Boore and Atkinson (B-A), Campbell and Bozorgnia (C-B), and Chiou and Youngs (C-Y), and the average shear wave velocity in the upper 30 meters of a soil column, V_{s30} , of 760 m/s to generate the 2008 seismic hazard maps for the Western United States. The results are being used to update the seismic design maps for use with the 2009 *NEHRP Provisions* and the 2010 ASCE Standard 7.

The site-response model for each of the B-A, C-B and C-Y NGA relationships uses a different bedrock spectral intensity parameter (see later), which is different from S_s and S_1 used in the 2003 *NEHRP Provisions* and ASCE-7-05. We combined the site amplification factors from the three NGA relationships and presented the NGA-based factors as a function of parameters equivalent to S_s and S_1 , enabling the comparison between the NGA-based and NEHRP/ASCE-7 site amplification factors.

Three sections follow this introduction. The first section introduces the combinations of variables, such as magnitude, distance and V_{s30} , considered in the study and the procedure we used to develop the average NGA-based site amplification factors, and discusses the source of the scatter in the developed factors. The second section presents the site amplification factors developed in this study and compares them with the corresponding NEHRP/ASCE-7 site class coefficients. The last section presents a summary and conclusions. More information is available in Huang et al. (2010).

Average NGA Site Amplification Factors

Combinations of Variables and Analysis Procedure

Table 1 lists the values of the parameters considered in the study: two types of faults, strike-slip (ss) and normal dip-slip (ds); moment magnitude (M_w) between 5 and 8; and closest site-to-source distance (r) between 0 and 50 km. The study focuses on sites with V_{s30} between 150 and 1500 m/s. Eight values of V_{s30} were considered: 1500 (Site Class A/B boundary per the *NEHRP Provisions* and ASCE-7), 1130 (midpoint of Site Class B), 760 (B/C boundary), 560 (midpoint Site Class C), 360 (C/D boundary), 270 (midpoint Site Class D), 180 (D/E boundary) and 150 (for Site Class E) m/s.

The output of the NGA relationships is a rotated geometric-mean spectral acceleration for two horizontal components of ground motion, termed GMRotI50 (Boore et al. 2006). For each combination of the variables identified in Table 1, the median estimate of GMRotI50 was computed using the B-A, C-B and C-Y NGA relationships. A site amplification factor for a given pair of period and V_{s30} was determined for each NGA relationship as the ratio of this GMRotI50 to the corresponding value at the B/C boundary ($V_{s30} = 760$ m/s). We report average NGA site amplification factors as the arithmetic mean of the ratios computed for each NGA relationship.

Table 1. Ground-motion parameters used in this study

Parameter	Unit	Cases or values for the parameter	Description
Fault type	--	strike-slip (ss) fault normal dip-slip (ds) fault	--
V_{S30}	m/s	1500, 1130, 760, 560, 360, 270, 180 and 150	Shear-wave velocity
M_W	--	5, 5.5, 6, 6.5, 7, 7.5, 8	Moment magnitude
r	km	0, 0.5, 1, 3, 5, 10, 15, 20, 30, 50	Closest site-to-fault distance
Dip	degree	=90 for ss fault =45 for ds fault	--

The variable “GMRotI50_{X,Y}” is used to present results. The subscript “X” denotes the period used to compute GMRotI50 and the subscript “Y” identifies the value of V_{S30} . For example, GMRotI50_{PGA,V760} is the rotated geometric-mean of PGA for $V_{S30} = 760$ m/s; and GMRotI50_{1s,V270}/GMRotI50_{1s,V760} is the ratio of the 1-second GMRotI50 for $V_{S30} = 270$ m/s to that for $V_{S30} = 760$ m/s, namely, the site amplification factor at the midpoint V_{S30} of Site Class D and a period of 1 second.

Figure 1 enables a comparison between the site amplification factors for the B-A, C-B and C-Y NGA relationships and the average NGA factors calculated in this paper. The site amplification factors presented in Figure 1 are for $V_{S30} = 270$ m/s at periods of 0.2 (panel a) and 1 (panel b) second and are plotted as a function of GMRotI50_{0.2s,V760} and GMRotI50_{1s,V760}, respectively. For each average NGA factor presented in Figure 1a (Figure 1b), the corresponding value of GMRotI50_{0.2s,V760} (GMRotI50_{1s,V760}) used for the abscissa is the average of those values computed using the B-A, C-B and C-Y NGA relationships for the scenario used to compute the average NGA factor. The results of Figure 1 show that the average NGA factors reasonably represent the trends of the site amplification factors for the three NGA relationships. In this study, only average NGA results are used to evaluate the NEHRP/ASCE-7 site class coefficients.

Scatter in the Data

The results of Figure 1 show some scatter in the relationships between site amplification factor (ordinate) and spectral acceleration (abscissa). The sources of the scatter are discussed below. The site amplification factors of Figure 1b were re-plotted as a function of both GMRotI50_{1s,V760} and GMRotI50_{PGA,V760} in panels a and b of Figure 2, respectively. A smaller range for the Y axis is used in Figure 2 to clearly show the distribution of the site amplification factors. In panel a, scatter is associated with the B-A and C-B models. In panel b, scatter is observed only for the C-Y model. This switch in scatter between the models results from the use of different bedrock spectral intensity measures for site amplification in the three NGA relationships.

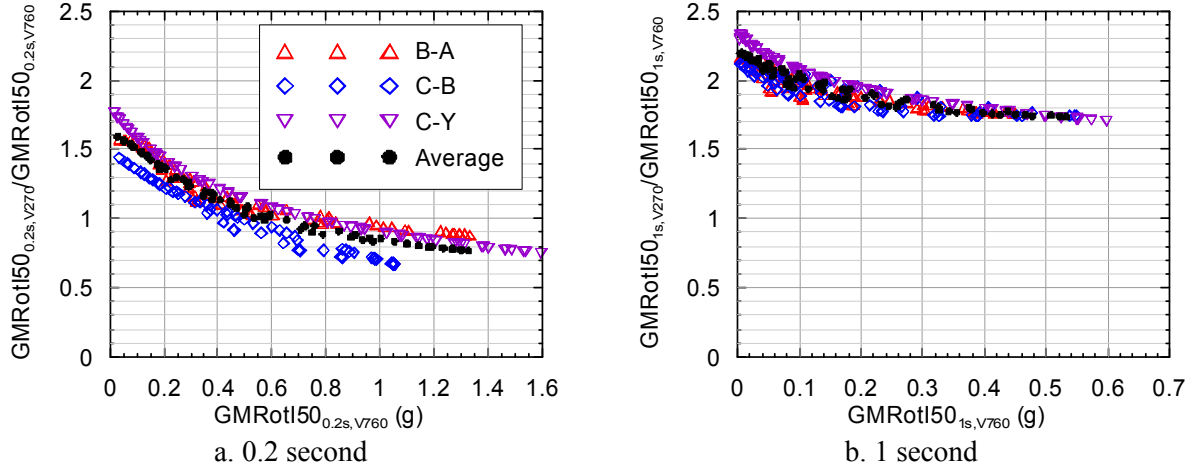


Figure 1. Site amplification factors for Site Class D (midpoint, $V_{S30} = 270$ m/s) at periods of a) 0.2 and b) 1 second using the attenuation models of Boore and Atkinson (2008), Campbell and Bozorgnia (2008) and Chiou and Youngs (2008), and the average of the factors across the three NGA models

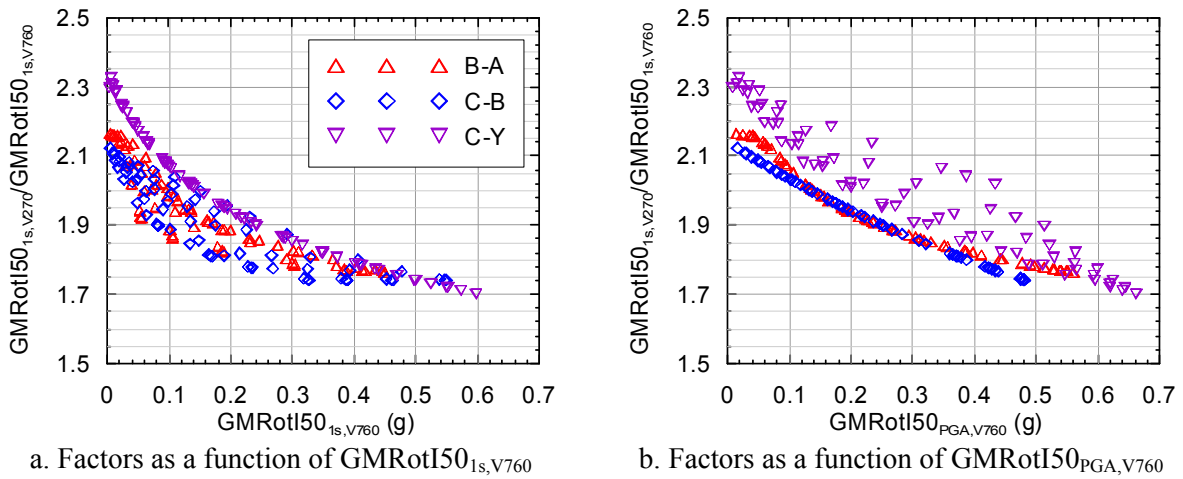


Figure 2. Site amplification factors for Site Class D (midpoint, $V_{S30} = 270$ m/s) at a period of 1 second as a function of a) $\text{GMRotI50}_{1s, V760}$ and b) $\text{GMRotI50}_{\text{PGA}, V760}$ using the attenuation models of Boore and Atkinson (2008), Campbell and Bozorgnia (2008) and Chiou and Youngs (2008)

For the B-A model, the site amplification factor, which is dependent on V_{S30} and period (T_i), is a smooth and continuous function of $\text{GMRotI50}_{\text{PGA}, V760}$ and is not directly dependent on magnitude, distance and fault type. That is, two different combinations of magnitude, distance and fault type (e.g., [7.5, 5 km, ss] and [6.5, 1 km, ds]) that return the same value of $\text{GMRotI50}_{\text{PGA}, V760}$ (e.g., 0.35 g) will have the same site amplification factor (e.g., 1.8 for $V_{S30} = 270$ m/s and a 1-second period). Therefore, there is no scatter in the B-A data of Figure 2b. Conversely, two different combinations of magnitude, distance and fault type that return the same value of $\text{GMRotI50}_{1s, V760}$ will generally produce different values of $\text{GMRotI50}_{\text{PGA}, V760}$ (see Figure 3a for the values of $\text{GMRotI50}_{\text{PGA}, V760}$ and $\text{GMRotI50}_{1s, V760}$ predicted using the B-A

model for the magnitudes, distances and fault types of Table 1), and thus two different site amplification factors and two points (scatter) in the $\text{GMRotI50}_{1s,V760}$ -amplification factor space (see the scatter in the B-A data of Figure 2a).

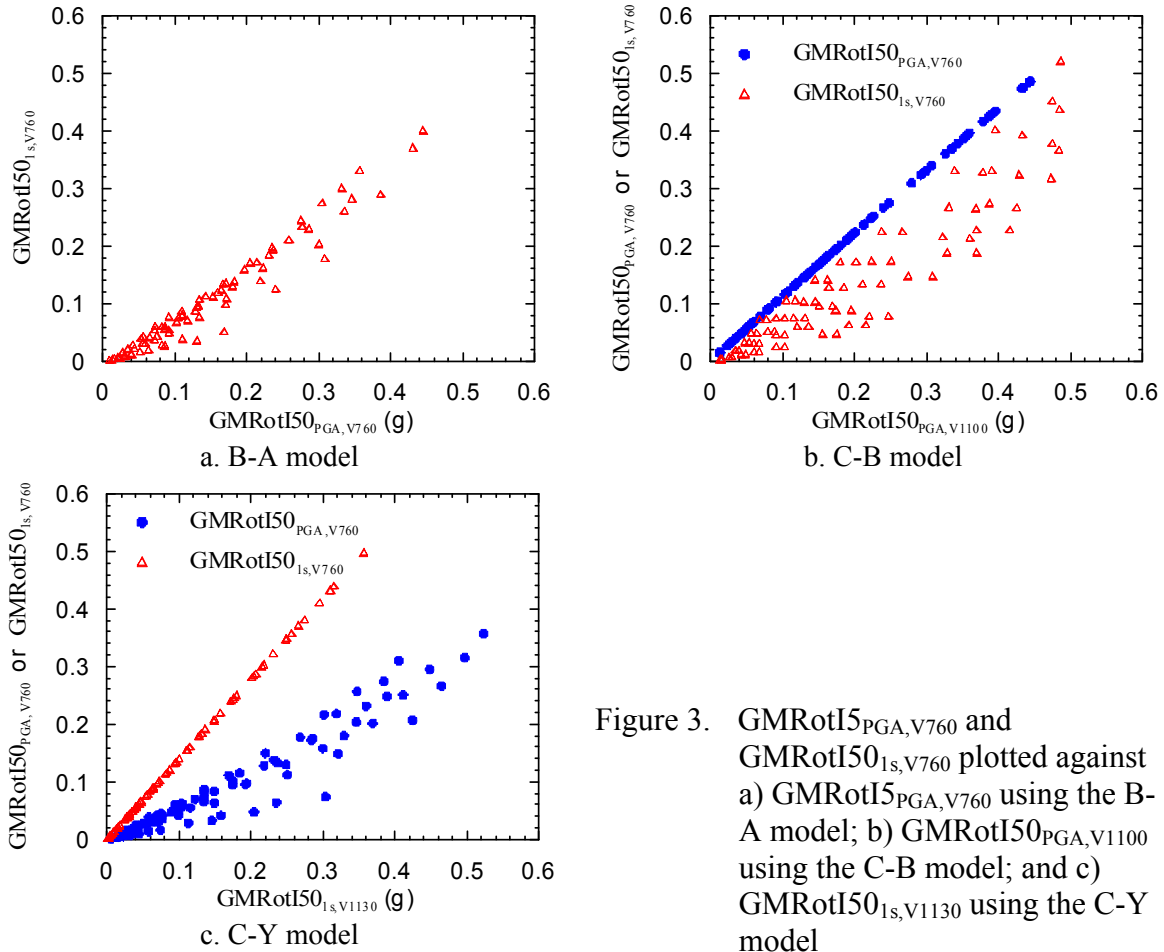


Figure 3. $\text{GMRotI50}_{\text{PGA},V760}$ and $\text{GMRotI50}_{1s,V760}$ plotted against a) $\text{GMRotI50}_{\text{PGA},V760}$ using the B-A model; b) $\text{GMRotI50}_{\text{PGA},V1100}$ using the C-B model; and c) $\text{GMRotI50}_{1s,V1130}$ using the C-Y model

For the C-B model, the site amplification factor for a given V_{S30} and T_i is a smooth continuous function of $\text{GMRotI50}_{\text{PGA},V1100}$. Figure 3b presents the values of $\text{GMRotI50}_{\text{PGA},V760}$ and $\text{GMRotI50}_{1s,V760}$ as a function of $\text{GMRotI50}_{\text{PGA},V1100}$ predicted using the C-B model for the magnitudes, distances and fault types of Table 1. The relationship between $\text{GMRotI50}_{\text{PGA},V1100}$ and $\text{GMRotI50}_{\text{PGA},V760}$ is linear but scatter is evident in the relationship between $\text{GMRotI50}_{\text{PGA},V1100}$ and $\text{GMRotI50}_{1s,V760}$, that is, a single value of $\text{GMRotI50}_{1s,V760}$ can be associated with multiple values of $\text{GMRotI50}_{\text{PGA},V1100}$ and thus multiple values of site amplification factor. As a result, the relationship between $\text{GMRotI50}_{\text{PGA},V760}$ and the site amplification factor for the C-B model has no scatter (see Figure 2b) but that between the site amplification factor and $\text{GMRotI50}_{1s,V760}$ does (see Figure 2a).

For the C-Y model, the site amplification factor at a given V_{S30} and T_i is a smooth continuous function of $\text{GMRotI50}_{T_i,V1130}$. Figure 3c presents the values of $\text{GMRotI50}_{\text{PGA},V760}$ and $\text{GMRotI50}_{1s,V760}$ as a function of $\text{GMRotI50}_{1s,V1130}$ predicted using the C-Y model for the

magnitudes, distances and fault types of Table 1. The scatter in the C-Y data of Figure 2 that appears in panel b but not in panel a can be explained using the results of Figure 3c as described above for the B-A and C-B models.

Analysis Results

Average NGA Site Amplification Factors as a Function of Period

Sample average NGA site amplification factors for Site Classes B, C, D and E and site class boundaries A/B, B/C, C/D and D/E are presented in Figure 4 as a function of period for ss faulting and two $[M_w, r]$ pairs: $[7.5, 1 \text{ km}]$ (panel a) and $[6, 30 \text{ km}]$ (panel b). The two combinations are selected to demonstrate typical trends in the average NGA site amplification factors at high and low values of spectral intensity. The values of $\text{GMRotI50}_{\text{PGA}, V1500}$ for the magnitude-distance pairs of panels a and b are 0.45 and 0.05 g, respectively.

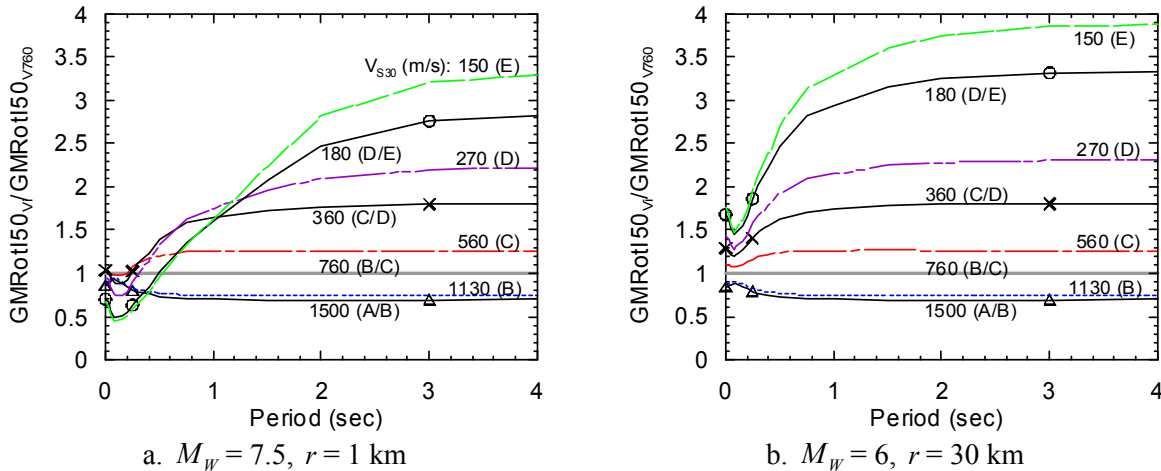


Figure 4. Average NGA site amplification factors versus period for $V_{s30} = 150, 180, 270, 360, 560, 760, 1130$ and 1500 m/s and a) $M_w = 7.5, r = 1 \text{ km}$ and strike-slip faulting, and b) $M_w = 6, r = 30 \text{ km}$ and strike-slip faulting

The key observations of Figure 4 are:

1. The site amplification factors for Site Classes B and C and boundaries A/B, B/C and C/D are essentially period-independent for periods greater than 1 second for both $[M_w, r]$ pairs,
2. The site amplification factors show a clear dependency on period for a) Site Classes D and E and the D/E boundary at all periods in panel a; and b) Site Classes D and E and boundaries C/D and D/E at periods smaller than 1 second in panel b. In panel a, the ratio of the site amplification factor at 0.5 (3) second(s) to that at 0.2 (1) second is 1.8 (1.7) at the D/E boundary and 1.9 (2.0) for Site Class E. In panel b, the ratio of the site amplification factor at 0.5 second to that at 0.2 second is 1.5 at the D/E boundary and 1.6 for Site Class E.

3. An increase in V_{S30} results in an increase of the site amplification factor at a given period for V_{S30} smaller than 360 m/s and periods smaller than 0.8 second in panel a. This trend in the site amplification factor for soft soil sites and high intensity bedrock shaking is seen in all three NGA models, was first identified by Borchardt (1994), and is captured by the NEHRP/ASCE-7 values for F_a for Site Classes D and E and S_s greater than 1 g.
4. The ratio of the site amplification factor at the D/E boundary to that at the C/D boundary at a period of 3 seconds is 1.5 in panel a and 1.8 in panel b. The results of Figure 4 show that the site amplification factor can vary significantly in the mid- and long-period ranges for a given bedrock spectral intensity and a site class (C, D or E).

Average NGA Site Amplification Factors and NEHRP/ASCE-7 Site Class Coefficients

The NEHRP/ASCE-7 site class coefficients are part of a *simplified* procedure to characterized free-field spectral demands and account for local soil conditions. For this purpose, Borchardt (1994) averaged site amplification factors over the short-period (0.1 through 0.5 second), intermediate-period (0.5 through 1.5 seconds), mid-period (0.4 through 2 seconds) and long-period (1.5 through 5 seconds) bands using Loma Prieta strong-motion records. Borchardt proposed that the four period bands be collapsed to two because factors in the intermediate-, mid- and long-period bands were similar. The NEHRP/ASCE-7 site class coefficients F_a and F_v were established from averages of the site amplification estimates in the short- and mid-period bands, respectively.

The NGA-based site amplification factors developed in this study (using the average of the factors for the three NGA models) were averaged over the short- and mid-period bands and compared with the NEHRP/ASCE-7 site class coefficients in Figure 5. For the short-period band, the factor was computed as the average of values at periods of 0.1, 0.2, 0.3, 0.4 and 0.5 second. The average of the values at periods of 0.4, 0.5, 0.75, 1, 1.25, 1.5, 1.75 and 2 seconds was taken as the mid-period band factor. The factors are plotted as a function of $GMRotI50_{0.2s, V760}$ (panels a, c and e) and $GMRotI50_{1s, V760}$ (panels b, d and f) to be consistent with the definition of S_s and S_1 in the 2003 *NEHRP Provisions* (ASCE-7), respectively. The s_s and d_s factors are not presented separately in each panel of Figure 5 since the trends for the two factors are nearly identical.

Panels a and b of Figure 5 present the average NGA site amplification factors for short- and mid-period bands, respectively, for Site Class C (midpoint) and the C/D boundary together with the corresponding NEHRP/ASCE-7 site class coefficients for Site Class C. The NEHRP/ASCE-7 F_a is most similar to the average NGA factors for Site Class C and the NEHRP/ASCE-7 F_v falls between the average NGA factors for Site Class C and the C/D boundary. The average NGA factors for Site Class C show smaller dependency on period than do the corresponding NEHRP/ASCE-7 site class coefficients.

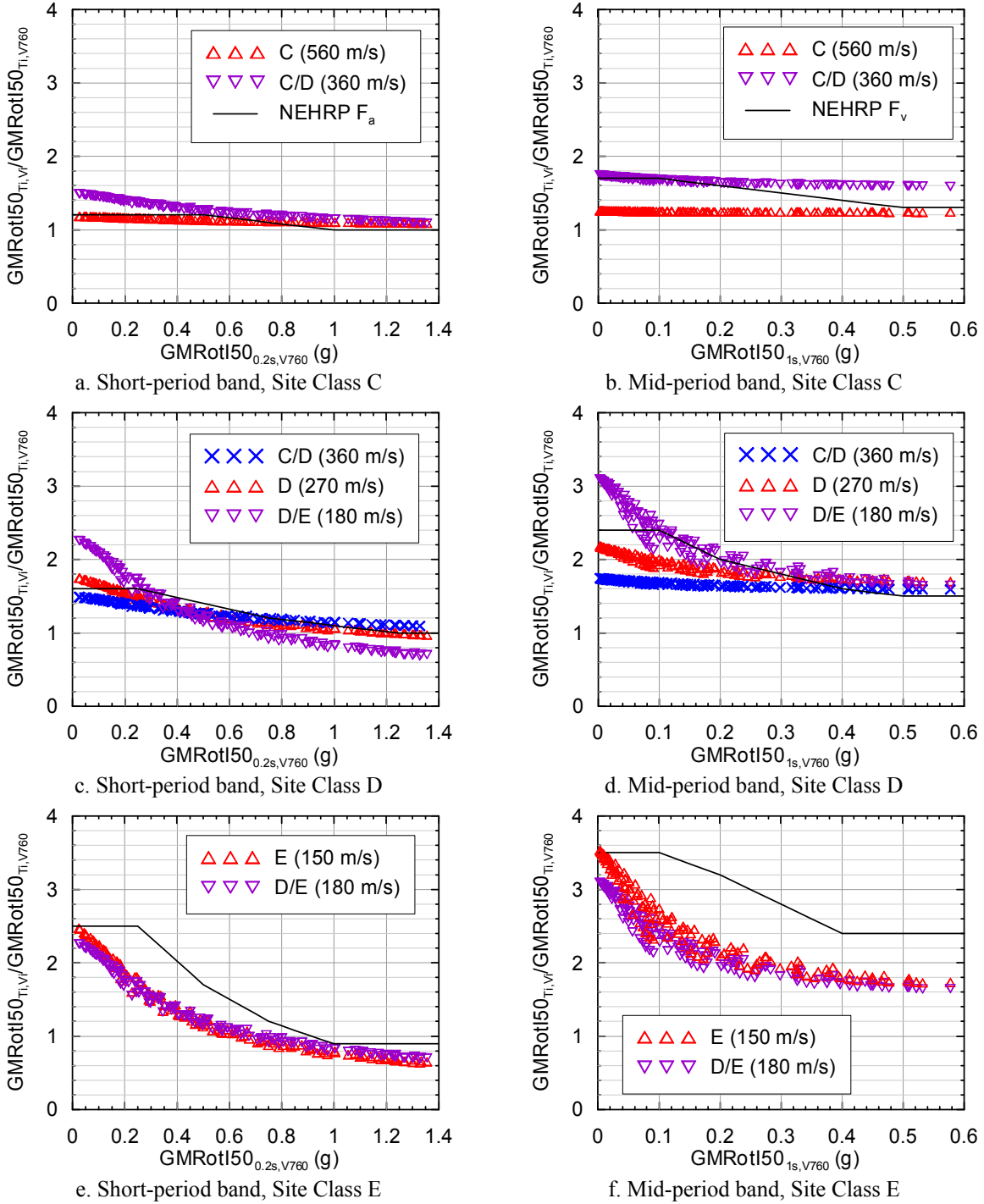


Figure 5. NGA-based site amplification factors for short- and mid-period bands for Site Classes C, D and E and the C/D and D/E boundaries, and NEHRP/ASCE-7 site class coefficients F_a and F_v for Site Classes C, D and E

Panels c and d of Figure 5 present the average NGA site amplification factors for short- and mid-period bands, respectively, for Site Class D (midpoint) and the C/D and D/E boundaries together with the corresponding NEHRP/ASCE-7 site class coefficients for Site Class D. The

NEHRP/ASCE-7 F_a is in good agreement with the average NGA factors for Site Class D. In panel d, the difference between the average NGA factors at Site Class D and the C/D and D/E boundaries is evident for $\text{GMRotI50}_{1s, V_{S30}}$ smaller than 0.1 g and decreases as the bedrock spectral intensity increases. The NEHRP/ASCE-7 F_v factors reasonably represent the amplitude and trends in the average NGA factors for Site Class D and at the D/E boundary, but less so at the C/D boundary.

Panels e and f of Figure 5 present the average NGA site amplification factors for short- and mid-period bands, respectively, for Site Class E (150 m/s) and the D/E boundary together with the corresponding NEHRP/ASCE-7 site class coefficients for Site Class E. The differences between the average NGA factors for Site Class E and at the D/E boundary are insignificant in panel e and modest in panel f, since the difference in V_{S30} for the two conditions is only 30 m/s. The NEHRP/ASCE-7 site class coefficients in both panels are greater than the average NGA factors. In particular, the NEHRP/ASCE-7 F_a is about 40% to 50% greater than the average NGA factor for $\text{GMRotI50}_{0.2s, V_{S30}}$ between 0.2 and 0.5 g, and the NEHRP/ASCE-7 F_v is about 50% and 30% greater than the average NGA factors at $\text{GMRotI50}_{1s, V_{S30}}$ of 0.2 and 0.4 g, respectively. However, it must be noted that the dependence of the average NGA factors on period is substantial for Site Class E, as seen in Figure 4.

The site amplification factors vary significantly across the ranges of period and V_{S30} for Site Classes D and E. Based on these observations, we have proposed an alternate presentation for site amplification factors, suitable for inclusion in the *NEHRP Provisions* and ASCE-7, to address these dependencies. More information for the proposed factors can be found in Huang et al. (2010).

Summary and Conclusions

A site amplification study was performed using three NGA relationships. The study considered a) strike-slip and normal dip-slip faulting; b) moment magnitude between 5 and 8; c) site-to-source distance between 0 and 50 km; and d) eight values of V_{S30} between 150 and 1500 m/s. For each combination of these variables, the ratio of rotated geometric mean (GMRotI50) for the given V_{S30} to that at the B/C boundary (i.e., the site amplification factor) was generated using each of the three NGA relationships and the average of the ratios was computed and presented as a function of $\text{GMRotI50}_{0.2s, V_{S30}}$ and $\text{GMRotI50}_{1s, V_{S30}}$. The key conclusions of the study are:

1. The average NGA site amplification factors show a clear dependency on period for V_{S30} smaller than 270 m/s. For Site Class E, the ratio of the site factors at 0.5 and 0.2 second can be as high as 1.9 and that at 1 and 3 seconds can be as high as 2.
2. The value of the average NGA site amplification factor can vary significantly within a given site class (C, D or E) at a given period in the mid- and long-period ranges. The ratio of the site factors at the D/E and C/D boundaries varies between 1.5 and 2 at a period of 3 seconds.
3. The NEHRP/ASCE-7 site class coefficients reflect the amplitudes and trends of the average NGA site amplification factors for the short-period band for the midpoints of Site Classes B,

C and D but overestimate the factor for Site Class E (at a shear wave velocity of 150 m/sec). The site class coefficients also overestimate the average NGA factors for the mid-period band at the midpoints of Site Classes C and D and for Site Class E. The average NGA factors at a period of 0.3 (1) second can be used to characterize the average NGA factors for the short-period (mid-period) band.

Acknowledgements

The authors thank Stephen Harmsen of the USGS for providing the original Fortran codes for the three NGA relationships and Dr. Roger Borcherdt of the USGS for his thoughtful comments on this study. Financial support for the study described in this paper was provided in part by the United States Geological Survey (USGS), Award Number 08HQGR0017.

Reference

- American Society of Civil Engineers (ASCE). 2006. "Minimum design loads for buildings and other structures." *ASCE/SEI 7-05*, American Society of Civil Engineers, Reston, Virginia.
- Boore, D. M., and Atkinson, G. M. 2008. "Ground-motion prediction equations for the average horizontal component of PGA, PGV, and 5%-Damped PSA at spectral periods between 0.01 s and 10.0 s." *Earthquake Spectra*, 24(1), 99-138.
- Boore, D. M., Watson-Lamprey, J., and Abrahamson, N. A. 2006. "Orientation-independent measures of ground motion." *Bulletin of the Seismological Society of America*, 96(4A), 1502-1511.
- Borcherdt, R. D. (1994). "Estimates of site-dependent response spectra for design (methodology and justification)." *Earthquake Spectra*, 10(4), 617-653.
- Campbell, K. W., and Bozorgnia, Y. 2008. "NGA ground motion model for the geometric mean horizontal component of PGA, PGV, PGD and 5% damped linear elastic response spectra for periods ranging from 0.01 to 10 s." *Earthquake Spectra*, 24(1), 139-171.
- Chiou, B. S.-J., and Youngs, R. R. 2008. "A NGA model for the average horizontal component of peak ground motion and response spectra." *Earthquake Spectra*, 24(1), 173-215.
- Dobry, R., Martin, G. R., Parra, E., and Bhattacharyya, A. 1994. "Development of site-dependent ratios of elastic response spectra (RRS) and site categories for building seismic codes." *Proceedings, 1992 NCEER/SEAOC/BSSC Workshop on Site Response During Earthquakes and Seismic Code Provisions*, University of Southern California, Los Angeles, CA, also, National Center for Earthquake Engineering Research Special Publication *NCEER-94-SP01*, Buffalo, NY.
- Federal Emergency Management Agency (FEMA). 2004. "NEHRP recommended provisions for seismic regulations for new buildings and other structures." *Rep. No. 450-1/450-2*, FEMA, Washington, D.C.
- Huang, Y.-N., Whittaker, A. S., and Luco, N. 2010. "NEHRP Site Amplification Factors and the NGA Relationships." *Earthquake Spectra*, accepted for publication.
- Power, M., Chiou, B., Abrahamson, N., Bozorgnia, Y., Shantz, T., and Roblee, C. 2008. "An overview of the NGA project." *Earthquake Spectra*, 24(1), 3-21.
- Seed, R. B., Dickenson, S. E., and Mok, C. M. 1994. "Site effects on strong shaking and seismic risk; recent developments for seismic design codes and practice." *American Society of Civil Engineering Structures Congress*, 12, 573-578.